

Enhanced Electron Lifetimes in Dye-Sensitized Solar Cells Using a Dichromophoric Porphyrin: The Utility of Intermolecular Forces

Long Zhao,[†] Pawel Wagner,[†] Holly van der Salm,[‡] Keith C. Gordon,[‡] Shogo Mori,[§] and Attila J. Mozer^{*,†}

[†]ARC Centre of Excellence for Electromaterials Science, Intelligent Polymer Research Institute, University of Wollongong, Wollongong, NSW 2522, Australia

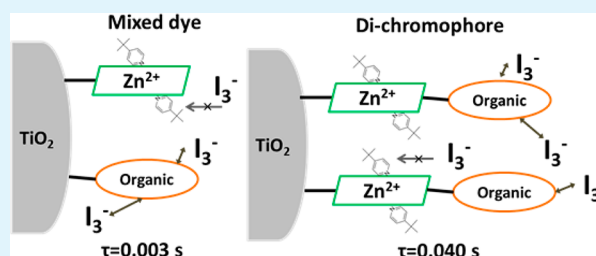
[‡]MacDiarmid Institute for Advanced Materials and Nanotechnology, Department of Chemistry, University of Otago, Dunedin 9016, New Zealand

[§]Division of Chemistry and Materials, Faculty of Textile Science and Technology, Shinshu University, Ueda, Nagano 386-8567, Japan

Supporting Information

ABSTRACT: Electron lifetimes in dye-sensitized solar cells employing a porphyrin dye, an organic dye, a 1:1 mixture of the two dyes, and a dichromophoric dye design consisting of the two dyes using a nonconjugated linker were measured, suggesting that the dispersion force of the organic dyes has a significant detrimental effect on the electron lifetime and that the dichromophoric design can be utilized to control the effect of the dispersion force.

KEYWORDS: porphyrin, organic dye, electron lifetime, intermolecular force, dye-sensitized solar cell



INTRODUCTION

Retardation of charge recombination between injected electrons and oxidized species of redox couples in dye-sensitized solar cells (DSSCs) is still an important issue especially when new redox couples are employed.^{1–3} The recombination can be retarded by surface treatment of the TiO₂ surface^{4–7} and by selecting an appropriate electrolyte to some degree.^{8–10} In addition, the electron lifetime has been controlled by tailoring the structure of dyes.^{2,11–14} The addition of alkyl chains to dyes is one of the typical strategies.¹⁵ As factors influencing the electron lifetime,¹³ we have proposed blocking effect, electrostatic force, and dispersion force. The dispersion force of dyes attracts redox couples in electrolyte solutions. Thus, when dyes having a larger dispersion force are employed in DSSCs, it results in faster recombination. The dispersion force is increased as the HOMO–LUMO energy gap of dyes is decreased.¹⁴ Thus, if dyes absorb a broad range of solar spectrum, the dyes attract redox species inherently.

While the effect of the dispersion force seems significant, it has not been taken into account explicitly to design new dyes. Previously, we reported that dimers, which consist of two porphyrin cores connected with a nonconjugated linker, gave longer electron lifetimes than porphyrin monomers.¹⁶ The longer electron lifetime was attributed to the addition of a blocking effect without increasing the dispersion force. In view of the light absorption property, the absorption spectrum of the dimer was similar to that of the monomer, and thus the optical benefit of the dimer was a higher absorption coefficient.¹⁷ In this work, we extend the idea of the nonconjugated dye design to obtain not only a longer electron lifetime, but also panchromatic absorption by synthesizing a dichromophoric

dye consisting of porphyrin and organic dye frameworks. We also demonstrate that this dichromophoric design can be utilized to control the effect of the dispersion force by comparison to individual and mixed monomers.

RESULTS AND DISCUSSION

Figure 1 shows the UV–vis absorption spectrum of the dyes measured in solution, together with their chemical structure. The synthesis and characterization (differential pulse voltammetry) of the organic dye 6 and dichromophoric dye 7 are reported in the Supporting Information, while detailed

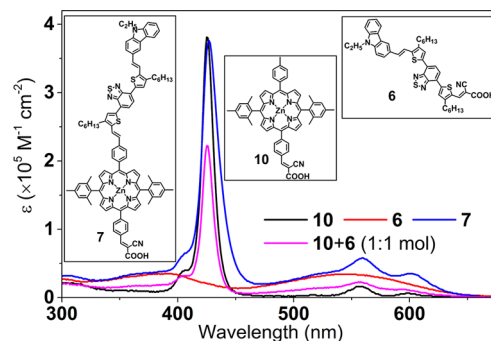


Figure 1. Molar extinction coefficient (ϵ) of the compounds measured in THF. The inset shows the molecular structure of the dyes.

Received: August 10, 2015

Accepted: September 16, 2015

Published: September 16, 2015

characterization of the porphyrin dye **10** has been reported elsewhere (see Table 1).¹¹ Organic dye **6** was selected for this study due to its lower onset of absorption (660 nm) and nearly twice as large extinction coefficient within the 450–650 nm wavelength range as compared to **10**, enabling increased light harvesting when used in a dichromophoric design. The porphyrin and organic dye chromophores are covalently attached using a phenylethenyl linker in **7**. As DFT calculations show (see Figures S4 and S5), the terthiophene unit of the side chain is twisted relative to the porphyrin plane by 64°, preventing the overlap of π orbitals. The lack of significant electronic communication in the ground state is evident from Figure 1 showing that the UV–vis absorption of **7** is a simple superposition of the spectrum of **10** and **6**. This is also consistent with DFT calculations (see Figures S4 and S5).

Figure 2 shows the current density versus applied potential curves for DSSCs prepared using **10**, **6**, and **7** and the mixture of **10** and **6** using thin, $2.0 \pm 0.1 \mu\text{m}$ transparent TiO₂ films. Measurements were recorded in the dark and under calibrated AM 1.5 100 mW cm⁻² white light illumination. The organic dye **6** and the **10+6** mixture (approximately 1:1 by mol on surface, 3:1 by mol in solution) achieves the highest short circuit current density (5.6 mA cm^{-2}), a 10% increase as compared to **10** and nearly twice as large as **7**. The open circuit voltage of DSSCs using the organic dye **6** is the lowest by 100 mV as compared to the porphyrin dye **10**. DSSCs using the **10+6** mixture show a 20 mV increase as compared to **6**, while the dichromophoric porphyrin dye **7** shows 20 mV lower V_{OC} as compared to **10**. The power conversion efficiency is between 2.3% and 2.4% for DSSCs sensitized by **10**, **6**, or the **10+6** dye mixture, while it is significantly lower at 1.4% for the DSSC sensitized by dye **7**.

Figure 3a shows the light harvesting efficiency (LHE) of DSSCs calculated using the absorption of the dye-sensitized thin film and an optical model.¹⁷ The dichromophoric dye **7** has the largest LHE across the whole visible wavelength spectrum peaking around 70%.

As compared to the LHE of **10**, the benefits of attaching the organic chromophore in **7** are evident both in a 2–3-fold increase in LHE values within the 500–650 nm wavelength range, as well as extending LHE by 40 nm to lower photon energies. In contrast, the improvement in LHE is less for the **10+6** mixed dye system. This is because the total dye loading by **10+6** is 30% less ($0.9 \times 10^{-4} \text{ mol cm}^{-3}$) as compared to **10**, **6**, and **7** ($(1.1\text{--}1.3) \times 10^{-4} \text{ mol cm}^{-3}$). By coadsorbing **10** and **6**, the individual chromophores are diluted, whereas using the dichromophoric dye design, the total chromophore concentration is doubled, clearly demonstrating the benefits of this approach when thin TiO₂ electrodes are used.

Figure 3b and c shows the IPCE and APCE = IPCE/LHE values. The highest peak IPCE values are measured for the porphyrin dye **10**. On the other hand, the organic dye **6** and the **10+6** mixed dye DSSCs show lower IPCE values but a broader wavelength coverage, giving the higher short circuit current densities as compared to **10**.

The IPCE values measured for **7** are less than one-half of **10** or **6**, and have a higher energy onset as compared to **6** and **10+6**. APCE, which in thin film devices with nearly 100% charge collection efficiency represents injection efficiency, is above 80% for **10** (see ref 11), 50% for **6**, 75% for **10+6**, and 30% for **7**. The APCE values are increased when using the same redox electrolyte without the *tert*-butylpyridine (*t*BP) additive (E2 electrolyte), causing a 100 mV shift in the open circuit

Table 1. Optical and Electrochemical Properties of the Compounds

	abs		DPV				J–V performance				τ (s) at ED = $1.5 \times 10^{18} \text{ cm}^{-3}$	
	λ_{max} (nm)	ϵ ($\times 10^5 \text{ M}^{-1} \text{ cm}^{-1}$)	λ_{onset} (nm)	$E_{\text{re}} (V \text{ vs } \text{Fc}^+)$	$E_{\text{ox}} (V \text{ vs } \text{Fc}^+)$	ΔE (eV)	J_{sc} (mA cm^{-2})	V_{OC} (mV)	FF	η (%)		dye loading ($\times 10^{-4} \text{ mol cm}^{-3}$)
10 ^a	426, 557, 599	3.80, 0.16, 0.07	620	–1.97	0.30, 0.59, 0.85	2.27	5.04	715	0.66	2.39	1.1	0.029
6 ^a	392, 548	0.35, 0.34	663	–1.62	0.30, 0.83	1.92	5.59	595	0.68	2.25	1.2	0.002
7 ^a	427, 560, 602	3.78, 0.58, 0.35	660	–1.67, –1.97	0.30, 0.40, 0.91	1.97	3.22	695	0.64	1.43	1.3	0.040
10+6 ^a (55:45 mol)	426, 558, 596	2.75, 0.19, 0.10	625				5.54	615	0.71	2.4	0.5 + 0.4	0.003
10 ^b							6.67	705	0.56	2.64	1.2	0.053
10 ^b							2.63	605	0.63	1	0.14	0.012
7 ^b							5.91	695	0.66	2.7	1.4	0.117
7 ^b							2.15	655	0.67	0.94	0.16	0.052

^aTiO₂ thickness, 2.2 μm . ^bTiO₂ thickness, 2.8 μm .

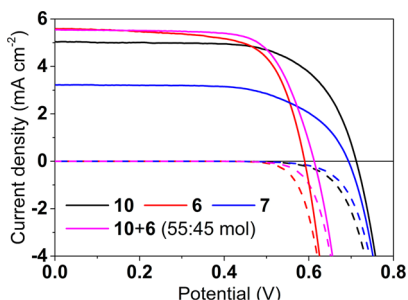


Figure 2. Current density–applied potential curves of DSSC measured under 100 mW cm^{-2} white light (solid lines) and dark (dashed lines). DSSCs were fabricated using $2.0 \pm 0.1 \mu\text{m}$ TiO_2 films.

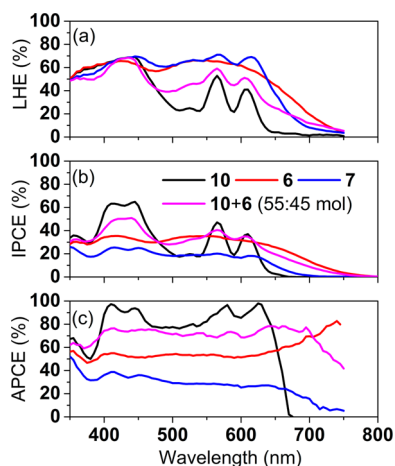


Figure 3. (a) Light harvesting efficiency (LHE), (b) incident photon to converted electron (IPCE), and (c) absorbed photon to collected electron (APCE) spectra of DSSCs using $2.0 \pm 0.1 \mu\text{m}$ TiO_2 films.

voltage versus charge density plots (see Figures S8 and S9), suggesting that the TiO_2 conduction band edge has shifted positively in agreement with numerous reports in the

literature.^{8,12,18–20} A downward shift in the CB edge position leading to increased injection efficiency¹² is the most likely cause for the increased IPCE values. The first reduction potential of 6 and 7 is 300 mV more positive as compared to 10, which suggests the more pronounced increase in IPCE of 6 and 7 using the E2 electrolyte is due to insufficient energy difference between the TiO_2 conduction band bottom edge potential and the reduction potential of the photo-excited dye 7 (Table 1). The low IPCE of 7 even using electrolyte E2 can be explained by the unfavorable electronic structure, that is, the side chain chromophore acting as an electron acceptor when the porphyrin core is photoexcited, creating a competing charge separation pathway to electron injection into TiO_2 (see Figure S8).

Figure 4 shows the electron lifetime and diffusion coefficient values determined using transient photovoltage and photocurrent decay measurements, together with using a charge extraction technique to obtain charge density at open circuit voltage condition. An order of magnitude longer electron lifetime was observed at matched electron density in DSSCs using 10 as compared to 6 (Table 1). The difference is mainly due to the ability of complex formation for the porphyrin with *t*BP; that is, the *t*BP could increase the blocking effect and/or reduce the effect of dispersion force of the porphyrin. When *t*BP was removed from the electrolyte, the lifetimes became comparable between the two dyes (see Figure S9). The mixed dye system 10+6 shows only a factor of 2 increase in electron lifetime as compared to 10. The electron lifetime in the mixed dye system appears to be less sensitive to the mixing ratio at lower concentrations of the porphyrin dye 10:6 (15:85, 25:75, 55:45; see Figure S6), with a slight increase when 10 is more than 50%. Because 6 attracts redox species strongly, the effect of 6 still dominates the electron lifetime. The dichromophoric dye 7 has the longest electron lifetime with a slight increase as compared to 10. The V_{OC} versus electron density plot shows a less than 50 mV shift. The difference in free energy cannot explain the order of magnitude difference in electron lifetime using the dichromophoric design. Dispersion force is caused by

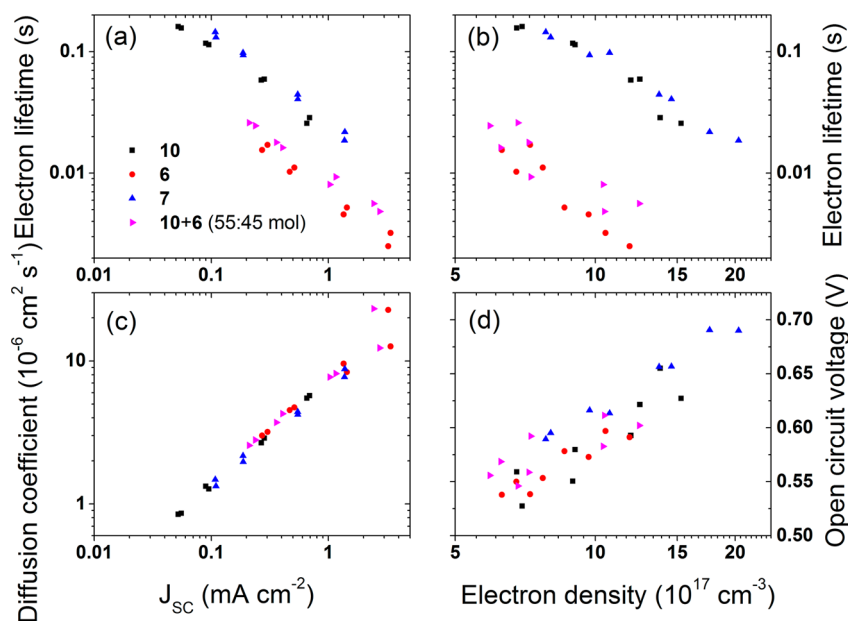


Figure 4. “Full” dye loading experiments: (a) electron lifetime and (c) diffusion coefficient versus short circuit current density, and (b) electron lifetime and (d) open circuit voltage versus electron density for DSSCs using the E1.

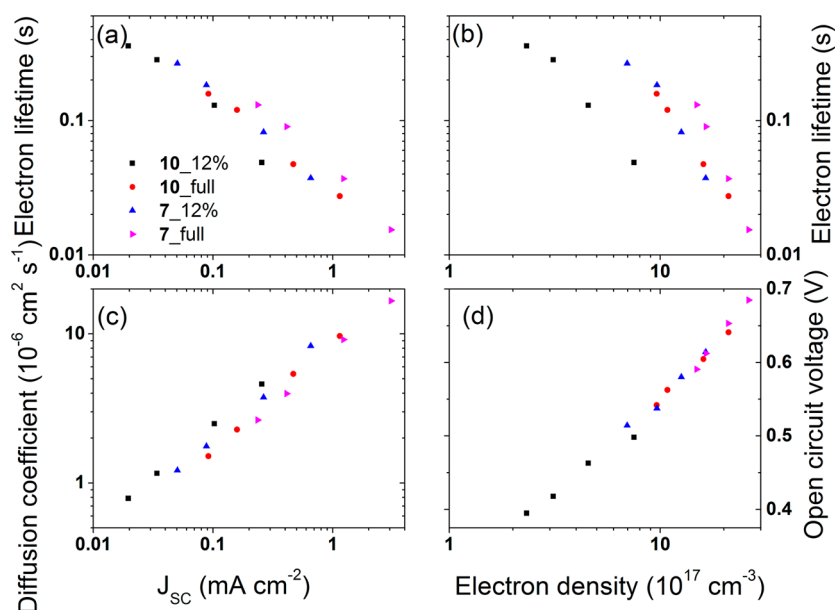


Figure 5. Reduced dye loading experiments: (a) electron lifetime and (c) diffusion coefficient versus short circuit current density, and (b) electron lifetime and (d) open circuit voltage versus electron density for DSSCs using the E1.

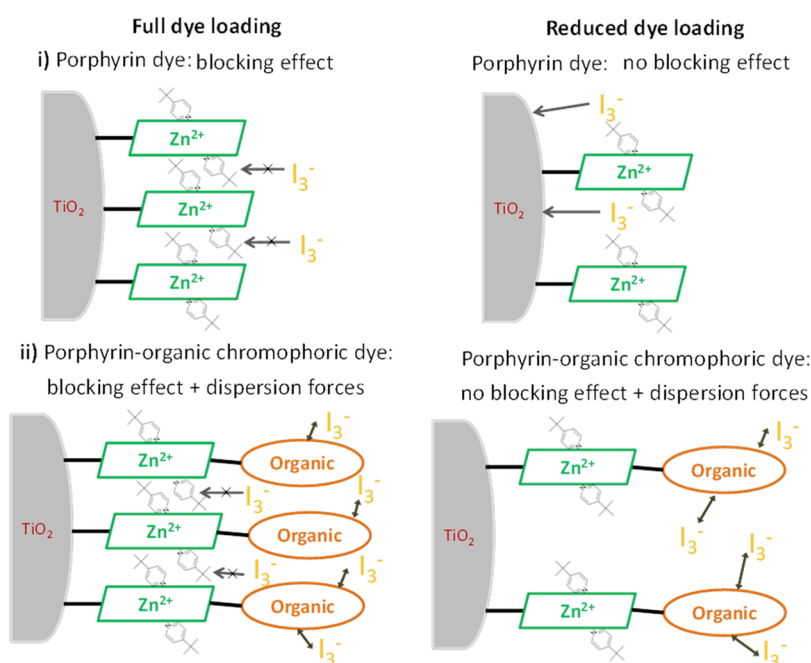


Figure 6. Graphical illustration of the effect of (i) physically blocking the approach of triiodide ions by *t*BP attracted to the Zn porphyrin and (ii) dispersion force by the organic chromophore at "full" and reduced dye loadings.

the induced dipole moment of molecules. The dichromophoric dye can have induced dipole moment in each chromophore; that is, two dipole moments can be formed in 7. The longest lifetime with 7 suggests that the effect of the two dipole moments can be controlled individually. The effect of the dispersion force due to the porphyrin core can be reduced by *t*BP in electrolyte, but the force due to the organic framework chromophore is fully effective. Because the organic chromophore is attached on the opposite side to the TiO₂ binding group of the porphyrin core, even though the thiophene-based chromophore attracts redox species, the attracted species are located a few nanometers away from the surface of the TiO₂. Thus, less facilitation of recombination is expected. The organic

chromophore can even block the diffusion of the redox species closer to the surface of the TiO₂, opening the possibility to utilize the dispersion force to elongate the electron lifetime.

To test the above hypothesis, electron lifetimes at reduced dye loading were compared in DSSCs using 10 and 7 (Figure 5). A new batch of TiO₂ films with slightly larger thickness (2.8 μm) was used for these experiments, which resulted in a higher short circuit current density and only small changes in the open circuit voltage at "full" dye loading conditions (Table 1). As the dye loading is reduced to 12% of the "full" loading condition, the short circuit current and the open circuit voltage for both 10 and 7 drop. Despite the nearly identical short circuit current at these reduced dye loading conditions, the open circuit

voltage obtained using **7** is 50 mV higher than that of **10**. Figure 5b suggests that the higher V_{OC} is due to the 5 times longer electron lifetime at reduced dye loading using **7** as compared to **10** at the same electron density (Table 1). The TiO_2 conduction bottom edge potential remains the same (no shift in electron density versus V_{OC}) as shown in Figure 5d. The important result is that the electron lifetime using **10** is greatly reduced at reduced dye loading, consistent with our previous explanation of blocking effect of bulky *t*BP molecules attracted to the Zn porphyrin molecule. At reduced dye loading, the blocking effect is expected to diminish as the now exposed TiO_2 surface cannot be effectively blocked by the much fewer molecules on the surface. In contrast, the electron lifetime at reduced dye loadings using **7** remained long. This is consistent with the proposed dispersion force acting between the organic chromophore and triiodide ions. The presence of the largely polarizable organic molecules a few nanometers away from the TiO_2 interface, even at low concentrations, is effective to locate triiodide ions away from the interface and therefore reduce the electron transfer rate between TiO_2 electrons and triiodide ions. The proposed mechanisms are displayed graphically in Figure 6. The above experiments, while not specifically probing the interaction between the dye molecules and triiodide ions, provide a very useful practical guide to increasing electron lifetime using low bandgap, hence highly polarizable chromophores using the dichromophoric concept. While the power conversion efficiencies of the dyes are not particularly high, the concept could be applied to much more broad absorption, champion DSSC sensitizers based on porphyrin and phthalocyanine dyes with large extended π -conjugation systems.

CONCLUSION

In summary, dye-sensitized solar cells were prepared with a porphyrin dye, an organic dye, the two dyes, or a dichromophore synthesized with the two dyes' frameworks with a nonconjugated linker. The electron lifetimes in the DSSCs were measured, showing the dyad and the organic dye gave the longest and the shortest lifetimes, respectively, while the porphyrin dye provided a slightly shorter electron lifetime than the dyad and the mixed dyes displayed a slightly longer electron lifetime than the organic dye. The results are explained by the organic dye having a larger attractive force to acceptor species in the electrolytes than the porphyrin dye. When the organic dyes are on the TiO_2 surface, they increase the concentration of the acceptor species in the vicinity of the TiO_2 surface. For the dyad, the organic dye component is attached on the top of the porphyrin dye, and thus the attracted acceptor species by the organic dye component are located far from the TiO_2 surface. This hypothesis is consistent with electron lifetime measurements at reduced dye loadings, which shows a large decrease of the electron lifetime measured for **10**, consistent with diminishing blocking effect, while it remains relatively long for **7**. Such interpretation leads to a design guide for such dyes; that is, the addition of the acceptor attraction center to dyes can be utilized to control the recombination, and organic dyes can be used as the attraction center.

EXPERIMENTAL SECTION

The synthesis and chemical analysis of the compounds are found in the Supporting Information.

UV-visible (UV-vis) absorption spectroscopy was recorded using a Shimadzu UV-3600 spectrophotometer in tetrahydrofuran (THF, 99.99%, Honeywell) solution at room temperature.

Dye-Sensitized Solar Cells (DSSCs) Fabrication and Characterization. The photoanode consisted of a fluorine doped tin oxide glass (FTO glass, 3 mm, $8 \Omega/\square$, Nippon Sheet Glass) substrate, spray-coated titanium diisopropoxide bis(acetylacetonate) (TAA, 75% in isopropanol, Aldrich) as a dense TiO_2 layer, screen-printed mesoporous TiO_2 layer (18-NRT, Dyesol), and a $TiCl_4$ solution (99.0%, Sigma-Aldrich) post-treatment as the mesoporous layer.¹¹ The size of each device active area was 4 mm \times 4 mm. The photocathode was a thermally decomposed Pt layer on FTO glass (2.2 mm, $7 \Omega/\square$, TEC).

The photoanodes were immersed into a dye solution for 1.5 h to achieve dye-sensitization. The solvent was THF (97%, Ajax), which was dried by activated alumina. The concentration of the dyes **10**, **7**, and **6** was 0.2 mM for the "full" dye loading condition. For the mix dye devices consisting of **10** and **6**, three different mole ratios were selected with the total dye concentration of 0.2 mM. The concentrations of **10** and **6** in the 1:3, 1:1, and 3:1 mixtures were 0.05 and 0.15, 0.1 and 0.1, and 0.15 and 0.05 mM, respectively. For the reduced dye loading in Figure 5, the photoanodes were immersed into a dye solution with the concentration of 0.01 mM.

The mole ratio in the mixture given in Figure 1 and Table 1 was calculated for solutions, while for Figures 2–4 it refers to that on the TiO_2 film.

E1 electrolyte was comprised of 0.6 M 1,2-dimethyl-3-propylimidazolium iodide (DMPII, synthesized in house), 0.1 M LiI (99.9%, Aldrich), 0.05 M I_2 (99.99%, Aldrich), and 0.5 M *tert*-butylpyridine (*t*BP, 96%, Aldrich) in acetonitrile (AN, 99.8%, Sigma-Aldrich):valeronitrile (VN, 99.5%, Sigma-Aldrich) with a v/v ratio of 85:15. E2 electrolyte was the same as E1, except it did not contain *t*BP.

Current density–voltage (J – V) measurements were carried out using simulated 100 $mW\ cm^{-2}$ AM 1.5 matched white light using a solar simulator (Newport). A Keithley 2400 source measure unit was used for recording the current/voltage response. A 6 mm \times 6 mm shadow mask was used. The devices were light-soaked for 20 minutes before performing solar cell characterization and charge extraction measurements.²²

Incident photon-to-current conversion efficiency (IPCE) was measured using a QEX10 quantum efficiency measurement system (PV measurements). The illumination spot size was smaller than the active area of the devices.

Light harvesting efficiency (LHE) measurements of the sensitized films were calculated from the UV-vis absorption of the films, considering the reflection from both photoanode and photocathode, as well as the absorption of the electrolyte.^{17,21}

Absorbed photon-to-current conversion efficiency (APCE) was calculated according to eq 1:

$$APCE(\lambda) = \frac{IPCE(\lambda)}{LHE(\lambda)} \quad (1)$$

Stepped light-induced measurements of photocurrent and photovoltage (SLIM-PCV) and charge extraction were carried out using the setup that was described elsewhere.^{11,12} A 635 nm diode laser was employed as the light source. Electron lifetime (τ) was measured by <1 mV voltage decay after stepping down the laser intensity at open circuit condition. Electron diffusion coefficient (D) was measured by <10% current decay after stepping down the laser intensity at short circuit condition. Electron density (ED) at open circuit condition was measured using a nanosecond switch (AsamaLab) by switching off the laser totally followed by accumulating the generated electrons using a multimeter (ADCMT 7461A).

The amount of dye loading on TiO_2 was determined by desorbing the dyes from the TiO_2 using 0.1 M tetrabutylammonium hydroxide solution (TBAOH, 40 wt % in water, Fluka) in DMF. The absorbance of the desorbed dye solution was to calculate the dye concentrations. For the mixed dye desorption studies, dye concentrations were

calculated from absorbance at 388 and 432 nm for the organic chromophore and the porphyrin, respectively.

■ ASSOCIATED CONTENT

Supporting Information

The Supporting Information is available free of charge on the ACS Publications website at DOI: 10.1021/acsami.5b07361.

Material synthesis, differential pulse voltammetry, detailed DFT calculations, and detailed photovoltaic characterization (PDF)

■ AUTHOR INFORMATION

Corresponding Author

*Tel.: +61242981429. E-mail: attila@uow.edu.au.

Notes

The authors declare no competing financial interest.

■ ACKNOWLEDGMENTS

A.J.M., K.C.G., P.W., and S.M. acknowledge support from the Australian Research Council (ARC) through Discovery Project no. DP110102201 and ARC Centre of Excellence for Electromaterials Science. A.J.M. acknowledges funding for Australian Research Fellowship (ARF). A.J.M. and P.W. acknowledge support from ANFF. H.v.d.S. and K.C.G. acknowledge the University of Otago and the MacDiarmid Institute for Advanced Materials and Nanotechnology for funding.

■ REFERENCES

- (1) O'Regan, B. C.; López-Duarte, I.; Martínez-Díaz, M. V.; Forneli, A.; Albero, J.; Morandeira, A.; Palomares, E.; Torres, T.; Durrant, J. R. Catalysis of Recombination and Its Limitation on Open Circuit Voltage for Dye Sensitized Photovoltaic Cells Using Phthalocyanine Dyes. *J. Am. Chem. Soc.* **2008**, *130*, 2906–2907.
- (2) Mozer, A. J.; Wagner, P.; Officer, D. L.; Wallace, G. G.; Campbell, W. M.; Miyashita, M.; Sunahara, K.; Mori, S. The Origin of Open Circuit Voltage of Porphyrin-Sensitized TiO₂ Solar Cells. *Chem. Commun.* **2008**, *0*, 4741–4743.
- (3) Yum, J.-H.; Baranoff, E.; Kessler, F.; Moehl, T.; Ahmad, S.; Bessho, T.; Marchioro, A.; Ghadiri, E.; Moser, J.-E.; Yi, C.; Nazeeruddin, M. K.; Grätzel, M. A Cobalt Complex Redox Shuttle for Dye-Sensitized Solar Cells with High Open-Circuit Potentials. *Nat. Commun.* **2012**, *3*, 631.
- (4) Palomares, E.; Clifford, J. N.; Haque, S. A.; Lutz, T.; Durrant, J. R. Control of Charge Recombination Dynamics in Dye Sensitized Solar Cells by the Use of Conformally Deposited Metal Oxide Blocking Layers. *J. Am. Chem. Soc.* **2003**, *125*, 475–482.
- (5) Fabregat-Santiago, F.; García-Cañadas, J.; Palomares, E.; Clifford, J. N.; Haque, S. A.; Durrant, J. R.; Garcia-Belmonte, G.; Bisquert, J. The Origin of Slow Electron Recombination Processes in Dye-Sensitized Solar Cells with Alumina Barrier Coatings. *J. Appl. Phys.* **2004**, *96*, 6903–6907.
- (6) Kopidakis, N.; Neale, N. R.; Frank, A. J. Effect of an Adsorbent on Recombination and Band-Edge Movement in Dye-Sensitized TiO₂ Solar Cells: Evidence for Surface Passivation. *J. Phys. Chem. B* **2006**, *110*, 12485–12489.
- (7) Kay, A.; Grätzel, M. Dye-Sensitized Core–Shell Nanocrystals: Improved Efficiency of Mesoporous Tin Oxide Electrodes Coated with a Thin Layer of an Insulating Oxide. *Chem. Mater.* **2002**, *14*, 2930–2935.
- (8) Nakade, S.; Kanzaki, T.; Kubo, W.; Kitamura, T.; Wada, Y.; Yanagida, S. Role of Electrolytes on Charge Recombination in Dye-Sensitized TiO₂ Solar Cell (1): The Case of Solar Cells Using the I-/I³⁺-Redox Couple. *J. Phys. Chem. B* **2005**, *109*, 3480–3487.

(9) Fabregat-Santiago, F.; Bisquert, J.; Garcia-Belmonte, G.; Boschloo, G.; Hagfeldt, A. Influence of Electrolyte in Transport and Recombination in Dye-Sensitized Solar Cells Studied by Impedance Spectroscopy. *Sol. Energy Mater. Sol. Cells* **2005**, *87*, 117–131.

(10) Ozawa, H.; YukiTawaray; Arakawa, H. Effects of the Alkyl Chain Length of Imidazolium Iodide in the Electrolyte Solution on the Performance of Black-Dye-Based Dye-Sensitized Solar Cells. *Electrochim. Acta* **2015**, *151*, 447–452.

(11) Zhao, L.; Wagner, P.; Elliott, A. B. S.; Griffith, M. J.; Clarke, T. M.; Gordon, K. C.; Mori, S.; Mozer, A. J. Enhanced Performance of Dye-Sensitized Solar Cells Using Carbazole-Substituted Di-Chromophoric Porphyrin Dyes. *J. Mater. Chem. A* **2014**, *2*, 16963–16977.

(12) Zhao, L.; Wagner, P.; van der Salm, H.; Clarke, T. M.; Gordon, K. C.; Mori, S.; Mozer, A. J. Dichromophoric Zinc Porphyrins: Filling the Absorption Gap between the Soret and Q Bands. *J. Phys. Chem. C* **2015**, *119*, 5350–5363.

(13) Miyashita, M.; Sunahara, K.; Nishikawa, T.; Uemura, Y.; Koumura, N.; Hara, K.; Mori, A.; Abe, T.; Suzuki, E.; Mori, S. Interfacial Electron-Transfer Kinetics in Metal-Free Organic Dye-Sensitized Solar Cells: Combined Effects of Molecular Structure of Dyes and Electrolytes. *J. Am. Chem. Soc.* **2008**, *130*, 17874–17881.

(14) Marinado, T.; Nonomura, K.; Nissfolk, J.; Karlsson, M. K.; Hagberg, D. P.; Sun, L.; Mori, S.; Hagfeldt, A. How the Nature of Triphenylamine-Polyene Dyes in Dye-Sensitized Solar Cells Affects the Open-Circuit Voltage and Electron Lifetimes. *Langmuir* **2010**, *26*, 2592–2598.

(15) Koumura, N.; Wang, Z.-S.; Mori, S.; Miyashita, M.; Suzuki, E.; Hara, K. Alkyl-Functionalized Organic Dyes for Efficient Molecular Photovoltaics. *J. Am. Chem. Soc.* **2006**, *128*, 14256–14257.

(16) Sunahara, K.; Griffith, M. J.; Uchiyama, T.; Wagner, P.; Officer, D. L.; Wallace, G. G.; Mozer, A. J.; Mori, S. A Nonconjugated Bridge in Dimer-Sensitized Solar Cells Retards Charge Recombination without Decreasing Charge Injection Efficiency. *ACS Appl. Mater. Interfaces* **2013**, *5*, 10824–10829.

(17) Mozer, A. J.; Griffith, M. J.; Tsekouras, G.; Wagner, P.; Wallace, G. G.; Mori, S.; Sunahara, K.; Miyashita, M.; Earles, J. C.; Gordon, K. C.; Du, L.; Katoh, R.; Furube, A.; Officer, D. L. Zn–Zn Porphyrin Dimer-Sensitized Solar Cells: Toward 3-D Light Harvesting. *J. Am. Chem. Soc.* **2009**, *131*, 15621–15623.

(18) Jennings, J. R.; Wang, Q. Influence of Lithium Ion Concentration on Electron Injection, Transport, and Recombination in Dye-Sensitized Solar Cells. *J. Phys. Chem. C* **2010**, *114*, 1715–1724.

(19) Boschloo, G.; Häggman, L.; Hagfeldt, A. Quantification of the Effect of 4-tert-Butylpyridine Addition to I⁻/I³⁺-Redox Electrolytes in Dye-Sensitized Nanostructured TiO₂ Solar Cells. *J. Phys. Chem. B* **2006**, *110*, 13144–13150.

(20) Kelly, C. A.; Farzad, F.; Thompson, D. W.; Stipkala, J. M.; Meyer, G. J. Cation-Controlled Interfacial Charge Injection in Sensitized Nanocrystalline TiO₂. *Langmuir* **1999**, *15*, 7047–7054.

(21) Kubo, W.; Sakamoto, A.; Kitamura, T.; Wada, Y.; Yanagida, S. Dye-Sensitized Solar Cells: Improvement of Spectral Response by Tandem Structure. *J. Photochem. Photobiol., A* **2004**, *164*, 33–39.

(22) Wagner, K.; Griffith, M. J.; James, M.; Mozer, A. J.; Wagner, P.; Triani, G.; Officer, D. L.; Wallace, G. G. Significant Performance Improvement of Porphyrin-Sensitized TiO₂ Solar Cells under White Light Illumination. *J. Phys. Chem. C* **2011**, *115*, 317–326.